

PLANT SCIENCES

Alternatives to photorespiration: A system-level analysis reveals mechanisms of enhanced plant productivity

Edward N. Smith^{1*†‡}, Marvin van Aalst^{2‡}, Andreas P. M. Weber³,
Oliver Ebenhöhn^{2,3}, Matthias Heinemann¹

Photorespiration causes a substantial decrease in crop yield because of mitochondrial decarboxylation. Alternative pathways (APs) have been designed to relocate the decarboxylation step or even fix additional carbon. To improve the success of transferring those engineered APs from model species to crops, we must understand how they will interact with metabolism and how plant physiology affects their performance. Here, we used multiple mathematical modeling techniques to analyze and compare existing AP designs. We show that carbon-fixing APs are the most promising candidates to replace native photorespiration in major crop species. Our results demonstrate the different metabolic routes that APs use to increase yield and which plant physiology can profit the most from them. We anticipate our results to guide the design of new APs and to help improve existing ones.

INTRODUCTION

Ribulose-1,5-bisphosphate carboxylase/oxygenase (rubisco) is the primary site of carbon fixation in plants. Alongside CO₂, rubisco can also react with oxygen to produce one molecule of 3-phosphoglycerate (3PGA) and one molecule of 2-phosphoglycolate (2PG). Through a process called photorespiration, the two-carbon product of the rubisco oxygenase reaction is converted back to an intermediate that can replenish the Calvin-Benson-Bassham cycle (CBB cycle). In this process, CO₂ and ammonia are released in the mitochondria and reassimilated in the chloroplasts. Photorespiration consumes adenosine 5'-triphosphate (ATP) and reducing power and causes losses of ~26% of fixed CO₂ and up to 36% of the yield of certain crops (1, 2). Thus, next to efforts in reducing the oxygenase activity of rubisco, the carbon and energy efficiency of photorespiration can be improved (2–5). This is highly desired to feed an increasing human population and to mitigate climate change.

Alternative pathways (APs) have been designed to increase the carbon and energy efficiency of photorespiration while still serving the primary function of photorespiration: detoxifying 2PG and replenishing the intermediates of the CBB cycle following the rubisco oxygenase reaction. There are four ways this can be achieved, ranging from fixing an additional CO₂ to two CO₂ per cycle being released (Fig. 1). For fixing additional carbon, the two-carbon 2PG can be converted into a three-carbon compound such as 3PGA by addition of one carbon from CO₂. A carbon-neutral photorespiratory pathway, with no net loss or fixation of CO₂, is accomplished by combining 2PG with other compounds to generate a four- or five-carbon compound that can replenish the CBB cycle directly. In partial decarboxylation pathways, such as native photorespiration, a 2PG molecule is decarboxylated to form a one-carbon compound

that can be combined with another 2PG to make a three-carbon compound that can enter the CBB cycle. Last, 2PG can be completely decarboxylated, releasing two CO₂ that can be refixed by the CBB cycle.

From a carbon perspective, an AP that fixes additional CO₂ would be preferred. However, additional carbon fixation comes along with extra energy and redox requirements, decreasing the supply for other cellular processes. In contrast, decarboxylation APs generate reducing power that can be captured as redox equivalents. In addition to that, decarboxylation APs can shift the rubisco activity toward carboxylation by releasing CO₂ in the chloroplast and thereby increasing the local concentration of CO₂. Thus, next to mere carbon efficiency, several other cellular parameters might determine the overall benefit of an AP.

Native photorespiration has cellular functions other than just clearing 2PG and replenishing the CBB cycle. Further functions include helping to balance ATP:NADPH supply and demand (6), increasing nitrogen assimilation into amino acids (7), and acting as an important source of 1C units (8) as well as serine and glycine (9). An ideal AP must therefore still support these other roles of native photorespiration.

All these aspects together indicate that implementing APs to photorespiration to accomplish increased crop yield is far from trivial. Simultaneously interfering with carbon, nitrogen, energy, and redox balances means interfering with a highly complex, intertwined system. Thus, whether any change increases or decreases crop yield is dependent on metabolism, physiology, and conditions, i.e., gas exchange differs with physiology and conditions and metabolism differs with conditions and growth stage/time of day etc. Toward rational engineering and full understanding of APs, global experimental analyses and mathematical modeling will likely be required to evaluate and understand the effect of variants. Exemplary for the challenge and for our yet limited understanding is the fact that we still do not fully understand the true cause for the increased yields observed in complete decarboxylation pathways that have been experimentally tested in plants (10).

In this work, we quantitatively examine 12 APs using different mathematical approaches (Fig. 1), building on previous modeling

Copyright © 2025 The Authors, some rights reserved; exclusive licensee American Association for the Advancement of Science. No claim to original U.S. Government Works. Distributed under a Creative Commons Attribution NonCommercial License 4.0 (CC BY-NC).

¹Molecular Systems Biology, Groningen Biomolecular Sciences and Biotechnology, 9747 AG Groningen, Netherlands. ²Institute of Theoretical and Quantitative Biology, Heinrich Heine University Düsseldorf, Düsseldorf, Germany. ³Institute of Plant Biochemistry, Cluster of Excellence on Plant Science (CEPLAS), Heinrich Heine University Düsseldorf, Düsseldorf, Germany.

*Corresponding author. Email: edward.smith@biology.ox.ac.uk

†Present address: Department of Biology, University of Oxford, Oxford, UK.

‡These authors contributed equally to this work.

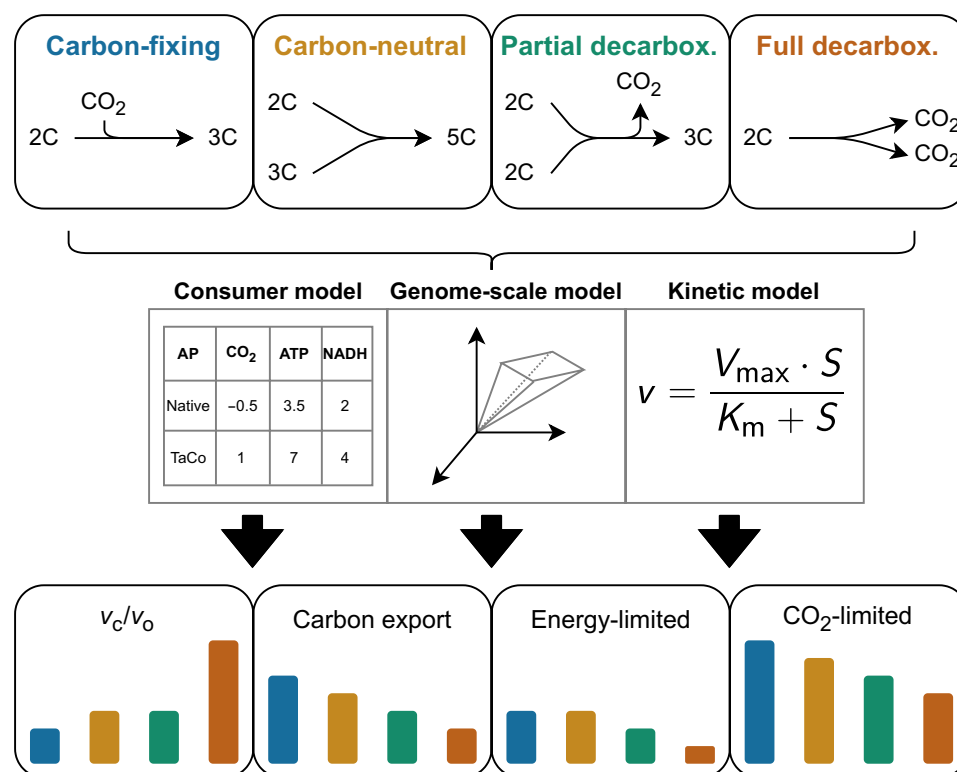


Fig. 1. Graphical overview of this work. We analyzed 12 alternative photorespiratory pathways that can be described using four general schemes regarding their carbon stoichiometry: carbon-fixing, carbon-neutral, partial decarboxylation, and full decarboxylation pathways. The three modeling approaches we used are a simple stoichiometric consumer model, a genome-scale model solved using flux balance analysis (FBA), and a kinetic model to describe key reactions with higher fidelity. Modeling at these different scales allowed the mechanisms behind potential alternative pathway (AP) benefits to be evaluated.

efforts (4, 10, 11). These APs include those that have experimentally been tested in planta but also include newly designed pathways that either are carbon neutral or fix additional CO_2 (11). Our assessment includes carbon efficiency, energy and redox effects, and effects emerging from altered subcellular CO_2 levels to make judgments on the yield increases that one can expect on the system level. In addition, we make predictions on optimal variants of AP designs (e.g., optimal enzyme location) and which types of plants might benefit the most from certain pathways and under which environmental conditions. By developing a mechanistic understanding of how APs can be effective, we identify the most promising pathways. Therefore, we hope to contribute to the challenge of increasing photosynthetic efficiency and, thus, crop yield to meet pressing societal issues.

RESULTS

Description of APs

Several APs have been proposed or implemented to date, which can be classified with regard to their CO_2 stoichiometry, ranging from fixing an additional CO_2 via being CO_2 neutral down to two molecules of CO_2 being released [see Fig. 2 and (4) for a review].

A CO_2 -fixing AP is the tartronyl-CoA (TaCo) pathway, which activates glycolate with CoA, carboxylates glycolyl-CoA to tartronyl-CoA, and then reduces tartronyl-CoA to generate glycerate (blue line in Fig. 2) (11, 12). The enzymes in the pathway and the metabolite tartronyl-CoA are not known to occur in nature, and therefore,

novel enzyme activities had to be engineered starting from related promiscuous enzymes. In particular, the glycol-CoA carboxylase, catalyzing the fixation of bicarbonate to form tartronyl-CoA, has been subject to multiple rounds of engineering to alter the kinetic properties and to reduce the futile hydrolysis of ATP (12, 13). While the TaCo pathway has been validated in vivo (12), it has yet to be tested in photosynthetic organisms.

Carbon-neutral pathways have been proposed on the basis of a glycolate reduction pathway, which converts glycolate to glycolaldehyde with glycolyl-CoA synthetase and glycolyl-CoA reductase, consuming ATP and NADPH (yellow lines in Fig. 2) (11). The glycolaldehyde is subsequently condensed with a sugar phosphate to generate longer-chain sugars or sugar phosphates that can re-enter the CBB cycle via further conversion steps. Four variants have been proposed depending on the intermediates generated, namely arabinose-5P, ribulose-1P, erythrose, or xylulose. These carbon-neutral pathways required the engineering of novel enzyme activities for the two steps of the glycolate reduction. These novel pathways have been validated in vivo (11) but are yet to be tested in photosynthetic organisms.

Partial decarboxylation pathways rely on combining two glycolate molecules and releasing one CO_2 to generate a three-carbon intermediate (green lines in Fig. 2). Several pathways with this design have been experimentally validated in plants. The pathways can be divided into those that rely on the *Escherichia coli* glycolate catabolic pathway of glyoxylate condensation via tartronic semialdehyde (Carvalho, Kebeish/South AP1, and Wang pathways) (5, 14–16) and

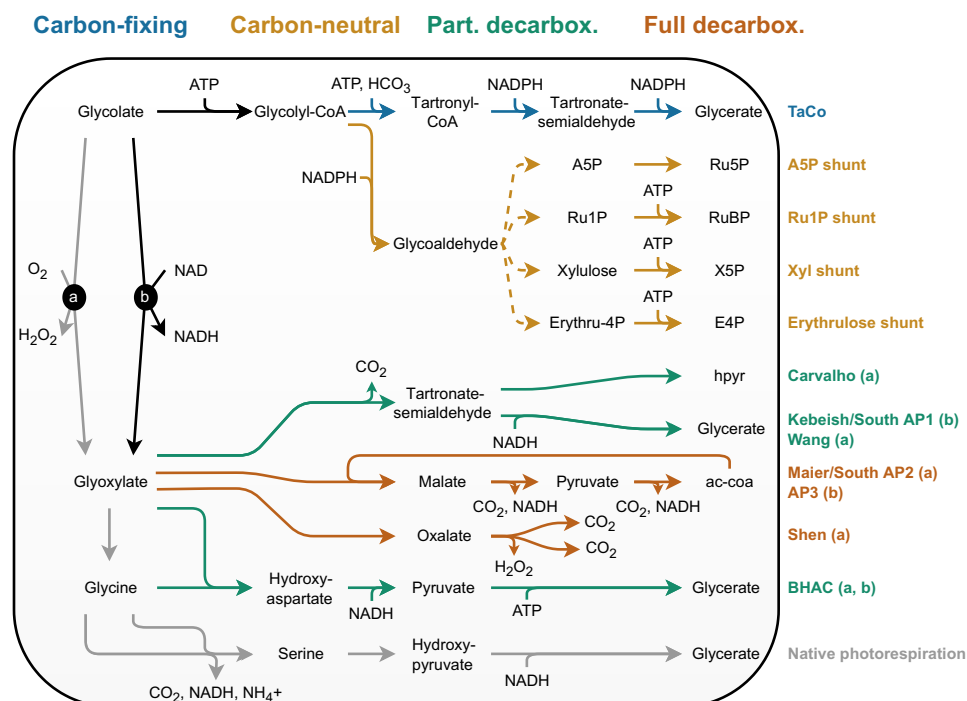


Fig. 2. Schematic depiction of alternative pathways (APs) studied in this work. Gray arrows indicate the reactions of native photorespiration, and colored arrows signify the classification regarding the carbon stoichiometry of the pathways: carbon-fixing, carbon-neutral, partial decarboxylation, and full decarboxylation pathways. Solid lines depict single reactions, while dashed lines depict intermediate steps that were omitted for clarity. The pathway variants a and b denote whether O₂/H₂O₂ or nicotinamide adenine dinucleotide (NAD)/NADH are used as the redox pair for glycolate dehydrogenase.

the β -hydroxyaspartate cycle (BHAC), which is the primary glycolate assimilation pathway in marine proteobacteria (17, 18). The tartronic semialdehyde-based pathway generates glycerate that can be phosphorylated and re-enter the CBB cycle. The Kebeish/South AP1 and Wang pathways have been implemented in chloroplasts, and the Carvalho pathway has been expressed in the peroxisome (perox). The BHAC pathway generates a 4C product from two glycolate molecules, oxaloacetate, which can directly be incorporated into biomass via aspartate or can be used to replenish the CBB cycle. For this, it must be decarboxylated to generate a three-carbon CBB cycle intermediate, for instance, 3PGA, via phosphoenolpyruvate-carboxykinase and enolase. So far, the BHAC pathway has been implemented in peroxisomes of *Arabidopsis* (17). The BHAC pathway could also theoretically be expressed in the plastid (plast), which would facilitate CO₂ reassimilation, but this remains to be tested in plants. The partial decarboxylation APs all release 0.5 CO₂ per rubisco oxygenase reaction, the same as in native photorespiration, but are proposed to be more energy efficient as they all avoid the release and subsequent re-fixation of ammonium.

Complete decarboxylation pathways convert glycolate to CO₂ using either malate synthase and pyruvate dehydrogenase (Maier/SouthAP2/AP3) (15, 19) or oxalate oxidase (Shen) (20) (dark orange lines in Fig. 2). The primary difference between the two options is the fate of reductant released from glyoxylate oxidation. Malate synthase generates NADPH and pyruvate dehydrogenase generates the reduced form of nicotinamide adenine dinucleotide (NADH), whereas in the oxalate oxidase pathway, two redox equivalents are transferred to water, generating two hydrogen peroxide (H₂O₂). The CO₂ released by glycolate decarboxylation can re-enter the CBB cycle and

therefore complete decarboxylation pathways can still fulfil the requirement of converting 2PG into a CBB cycle intermediate.

In both partial and complete decarboxylation APs and in native photorespiration, oxidation of glycolate is the first step (Fig. 2, A and B). Variants exist on in which subcellular compartment this oxidation takes place and on what the final electron acceptor is of the oxidation. In native photorespiration, the Carvalho pathway, and BHAC (perox) pathway, glycolate oxidase is located in the peroxisome and converts glycolate to glyoxylate, generating H₂O₂ (16, 17). In the Maier/South AP2, Shen, and Wang pathways, glycolate oxidase was relocated to the chloroplast, potentially altering subcellular redox dynamics (5, 15, 19, 20). Glycolate dehydrogenase from *E. coli*, which generates NADH, was used for the Kebeish and South AP1 pathways, and glycolate dehydrogenase from the algae *Chlamydomonas reinhardtii* (CrGDH), with a yet unknown electron acceptor, was used in the South AP3 pathway (15, 21). The different electron acceptors of the glycolate oxidation reaction have effects on the energy state and redox metabolism in the chloroplast, potentially affecting stress responses to high light. Overall, the above-described APs all convert 2PG to a CBB cycle intermediate. Yet, they differ in the CO₂ stoichiometry, the energetic and redox costs, and their subcellular location.

A consumer model allows comparison of AP stoichiometries

To compare the ATP, redox equivalents, and CO₂ stoichiometry of the CBB cycle, photorespiration, and APs, it is convenient to define the pathways as closed cycles that regenerate one molecule of ribulose-1,5-bisphosphate (RuBP) and fix or release CO₂ and triose phosphates in a so-called consumer model (11). In this way, photorespiration can

be separated from the CBB cycle to directly compare energy and CO₂ stoichiometries. To calculate the ATP, redox equivalents, and CO₂ costs of the APs, the individual reaction steps starting and ending at RuBP were summed (Table 1).

The three complete decarboxylation pathways, South AP3, Maier/South AP2, and Shen, require the same amount of ATP but differ in their redox equivalent stoichiometry, e.g., production of H₂O₂ or NAD(P)H (Table 1). Here, and in subsequent analyses, we assumed that the CrGDH used in the South AP3 pathway indirectly produces NADH, although the exact electron acceptor remains unknown (21). The South AP3 and Maier/South AP2 pathways have the lowest total energy costs because they net generate NAD(P)H from the decarboxylation of glycolate (Table 1). Compared to native photorespiration, the partial decarboxylation pathways BHAC (perox), Carvalho, and Wang save 0.5 ATP and 0.5 NADPH by avoiding ammonia release but require an additional NADH for reduction of tartronic-semialdehyde and do not gain 0.5 NADH from the oxidation of glycine. Therefore, avoiding the cost of ammonium release in these pathways only saves 0.5 ATP per rubisco oxygenase conversion when compared to native photorespiration. The Kebeish/South AP1 and BHAC (plast) pathways have the same benefits from avoiding ammonia release but also produce an additional NADH from the use of glycolate dehydrogenase in place of the glycolate oxidase used by the Carvalho, Wang, and BHAC (perox) pathways. The carbon-neutral pathways require 0.5 to 1.5 more ATP than native photorespiration but require the same amount of redox equivalents (Table 1). The carbon-fixing TaCo pathway has the largest total energy cost as redox equivalents and ATP are required to fix CO₂ in this pathway (Table 1). Overall, there is a positive correlation between CO₂ released/taken up and the total energy cost of the pathway. Here, carbon-fixing pathways have the largest energy cost and CO₂-releasing pathways, which can generate redox equivalents from

the oxidation of previously fixed carbon, have the lowest energy cost.

The net-zero CO₂ consumer model accounts for the cost of CO₂ release

The previous consumer model does not account for the increase in energetic cost caused by CO₂ release, which needs to be refixed by the CBB cycle, or the reduction in energetic costs if CO₂ is fixed by the APs. Accounting for the cost of modified CO₂ stoichiometry provides a different perspective and allows for more direct comparison between pathways. For example, in native photorespiration, if we also account for the cost of fixing the additional 0.5 carbons required to compensate for the loss of CO₂ by glycine decarboxylase, then an additional cost of 1.5 ATP and 1 redox equivalent is required (with the simplifying assumption that the CBB cycle can fix CO₂ with no associated rubisco oxygenase or photorespiration). Therefore, the total cost for native photorespiration, assuming no net release/uptake of CO₂, is five ATP and three redox equivalents per regeneration of RuBP (Table 1). Similar calculations were performed for all APs. Note that for the TaCo pathway, which fixes one CO₂, we calculated a benefit in terms of ATP and NADPH spared by not requiring CBB cycle flux.

The complete decarboxylation pathways now have the largest total energy costs as an additional six ATP and four NADPH are required to refix the two CO₂ that are lost by these pathways (Table 1). The partial decarboxylation pathways have a small additional energy cost for refixation of 0.5 CO₂, and the carbon-neutral pathways have no additional costs/benefits as no additional CO₂ must be fixed. In contrast, the TaCo pathway spares three ATP and two NADPH as it fixes an additional CO₂, reducing the total energy cost. Overall, from an energetic perspective, the importance of accounting for CO₂ stoichiometry becomes apparent as large direct energy costs in CO₂-fixing pathways can be compensated for by the energy saving from additional CO₂ fixation.

Table 1. The consumer model allows comparison of alternative pathway (AP) stoichiometries. ATP, redox equivalent (eq.), and CO₂ stoichiometry of APs defined as converting 2PG to RuBP [extended from (4)]. Positive values represent consumption, and negative values represent production. The total energy cost assumes 2.5 ATP per redox equivalent. To account for differences in CO₂ stoichiometry, the energy costs for 0 net change in CO₂ were calculated by assuming that the CBB cycle can compensate for the release/uptake of CO₂ caused by photorespiration or APs. For example, for native photorespiration, an additional 1.5 ATP and 1 redox equivalent must be spent to compensate for the 0.5 CO₂ released. For the TaCo pathway, three ATP and two redox equivalents are spared as one CO₂ is already fixed by the AP.

AP	CO ₂	ATP	Redox eq.	Total energy cost	ATP at net-zero CO ₂	Redox eq. at net-zero CO ₂	Total energy cost at net-zero CO ₂
TaCo	1	7	4	17	4	2	9
Ara5P/Ru1P shunt	0	4	2	9	4	2	9
Xyl./eryth. shunt	0	5	2	10	5	2	10
BHAC (plast)	−0.5	3	1	5.5	4.5	2	9.5
Kebeish/South AP1	−0.5	3	1	5.5	4.5	2	9.5
BHAC (perox)	−0.5	3	2	8	4.5	3	12
Carvalho	−0.5	3	2	8	4.5	3	12
Wang	−0.5	3	2	8	4.5	3	12
Photorespiration	−0.5	3.5	2	8.5	5	3	12.5
South AP3	−2	2	−2	−3	8	2	13
Maier/South AP2	−2	2	−1	−0.5	8	3	15.5
Shen	−2	2	1	4.5	8	5	20.5
CBB cycle	1	3	2	8			

Stoichiometric network modeling accounts for system-wide effects of APs

While the consumer model offers a useful description of the pathway stoichiometries, it does not capture the interplay of APs with the wider metabolic network, such as amino acid metabolism. Therefore, we extended our analysis by integrating the individual APs in a large-scale stoichiometric model of core plant metabolism based on an *Arabidopsis* leaf, including photosynthetic electron transport and subcellular compartments (22). We used these models to investigate whether the APs can replace the complete flux of native photorespiration. Therefore, photorespiration was blocked by constraining the flux through glycine decarboxylase to zero. To ensure that flux through photorespiration or an AP was required, we mimicked ambient CO₂ partial pressure by fixing the rubisco carboxylase: oxygenase ratio at 3:1 (23).

Carbon-fixing APs are more energy efficient

We first assessed the photosynthetic energy efficiency of the APs, which we defined as the CO₂ fixed per photon absorbed. For this, a sink reaction for glyceraldehyde-3-phosphate (GAP) was fixed to 1 $\mu\text{mol s}^{-1}$ and the optimization objective was set to minimization of photon influx. Thus, the most energy-efficient flux distribution was identified for each AP.

The photosynthetic energy efficiency of the APs can have largely different values, ranging from a 27% increase down to a –54% decrease relative to native photorespiration (Fig. 3). The carbon-fixing TaCo pathway shows the largest increase, followed by the carbon-neutral Ara5P and xylulose APs (Fig. 3). The partial decarboxylation APs range from a small increase to almost no change, and the complete decarboxylation APs show a large decrease in photosynthetic energy efficiency (Fig. 3). In terms of energetic efficiency, the net carbon exchanged by the AP has the greatest effect, with carbon-fixing APs being the most energy efficient and decarboxylation APs being the least energy efficient (Fig. 3). The second most important factor determining the relative energy efficiency is the fate of redox equivalents or electrons from 2PG. Conversion of 2PG to CO₂ can generate three pairs of electrons that can be used to reduce either NAD(P)⁺ to generate redox equivalents or water to generate H₂O₂. APs that generate more NAD(P)H (Fig. 2 and Table 1) therefore have an advantage in terms of energy efficiency (Fig. 3).

APs can provide biosynthetic energy efficiency benefits

Photorespiration interacts with other metabolic pathways besides the CBB cycle. For example, carbon can be withdrawn from native photorespiration to provide one-carbon units (CH₂-THF), glycine, or serine, which can result in the release of less than 0.5 carbons per rubisco oxygenase reaction (9, 24–28). Similarly, intermediates can also be withdrawn from APs and used to synthesize amino acids or other biomass precursors. To calculate the impact that APs have on wider metabolism, we calculated the relative energy efficiency in the presence of APs with more complex cellular outputs including *Arabidopsis* phloem exudate or biomass (29, 30). In general, for the carbon-fixing, carbon-neutral, and Kebeish/South AP1 pathways, the benefit of the APs decreases as the output complexity increases (Fig. 3). Phloem exudate and biomass contain amino acids that can already be efficiently synthesized by native photorespiration. Therefore, the benefit of these APs is smaller when the cell is producing amino acids compared to GAP alone because these APs do not generate amino acids or

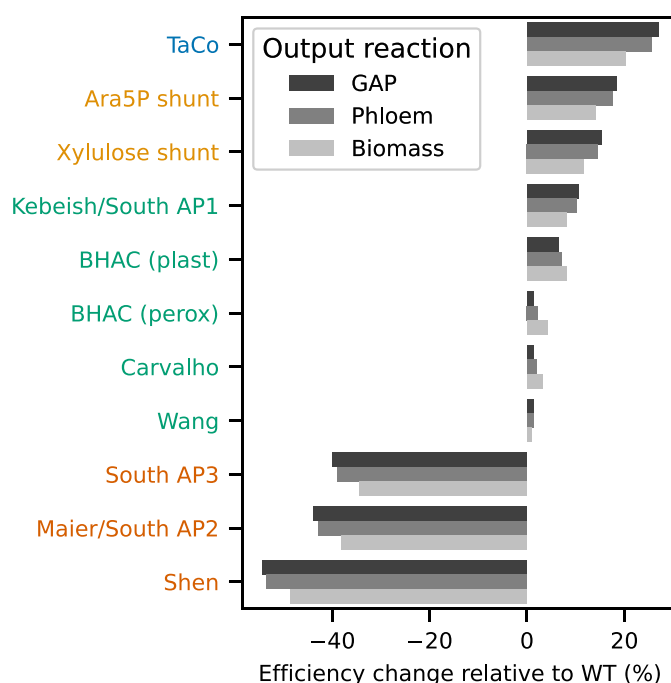


Fig. 3. Change in photosynthetic energy efficiency (CO₂ fixed per photon) of alternative pathways (APs) relative to wild-type (WT) photorespiration. Rubisco carboxylase:oxygenase ratio fixed at 3:1 and efficiency calculated by stoichiometric flux balance analysis (FBA) modeling. Negative numbers denote a decrease in CO₂ fixed per photon relative to the WT, while positive numbers denote an increase. Model outputs were fixed to either GAP, phloem exudate, or biomass represented by gray shading. AP label colors signify the amount of CO₂ the AP fixed or released by the APs. Blue, 1; yellow, 0; green, –0.5; orange, –2. For the absolute number of absorbed photons per CO₂ fixed, see fig. S2.

amino acid precursors as intermediates. In contrast, the BHAC and Carvalho pathways demonstrate an enhanced benefit when synthesizing biomass or phloem exudate compared to GAP alone (Fig. 3). The synthesis of amino acids with five-carbon backbones is more efficient in the presence of the BHAC and Carvalho pathways as additional separate decarboxylation steps and subsequent refixation of CO₂ are not required to synthesize these amino acids. Similarly, the complete decarboxylation pathways also show a benefit (i.e., decreased energy efficiency penalty) when synthesizing biomass or phloem exudate in comparison to just GAP alone (Fig. 3). Specifically, in the Maier/South AP2 and South AP3 pathways, carbon can be withdrawn as malate from malate synthase. Malate can then be used as the carbon backbone for generating aspartate and other derived amino acids. In this way, carbon is conserved and not released as CO₂ that must be refixed with an associated energetic cost.

APs can have some small additional benefits compared to native photorespiration when cells are synthesizing biomass, and these will depend on the precise amino acid demands of the leaf. The wild-type (WT) model predicts here that ~6% of the carbon entering native photorespiration is withdrawn as serine, substantially less than the 32% reported for tobacco leaves (9). All the APs investigated here bypass the serine-producing steps of native photorespiration and could therefore disadvantage the plant if serine is in high demand and other serine-producing pathways are unable to compensate. Overall, however, the greatest effect of the APs is on the efficiency of

carbon fixation and any changes in the energy efficiency of synthesizing biomass precursors are likely to be relatively minor.

APs alter the ATP and NADPH demand

If the linear electron flow of photosynthesis supplies a fixed stoichiometry of ATP and redox equivalents, then this may not necessarily match the demand of the cell. Plants use various mechanisms to match the supply to the demand, such as cyclic electron flow, but imbalances can potentially lead to photosynthetic inefficiency or damage (6). Introducing APs can alter the ATP and redox demands of the cell with potentially positive or negative effects. We therefore quantified the ratio of ATP to NADPH demand of the cell in the presence of the APs to see whether the demand is shifted toward or away from the ratio supplied by linear electron flow.

For this, we identified the most energy-efficient flux distribution by forcing a GAP outflux of $1 \mu\text{mol s}^{-1}$ while minimizing the photon input and then quantified the fluxes through ATP synthase and ferredoxin-NADP reductase to quantify the net ATP and reductant demand. Because the model represents autotrophic leaf metabolism, these reactions are the primary source of ATP and NADPH and can therefore be used to calculate the net ATP:NADPH demand of the cell.

Here, only the Carvalho, Wang, and peroxisomal BHAC pathways, with an ATP:NADPH demand of 1.5, are closer to the supply from linear electron flow (1.28) than that of a plant with WT photorespiration (1.56) (Fig. 4). The lower ATP:NADPH demand in the Carvalho, Wang, and BHAC (perox) pathways is due to avoiding the need for ammonia reassimilation and the associated ATP cost. APs that capture the redox equivalents from complete glycolate decarboxylation as NADPH, such as the Maier and South AP3 pathways, substantially increase the demand of ATP relative to NADPH (up to 2.75 in South AP3) (Fig. 4). This is caused by the increased NADPH supply from glycolate decarboxylation, which decreases NADPH that must be supplied from photosynthetic electron flow. In contrast, the Shen pathway, which also completely decarboxylates glycolate, does not capture the redox equivalents as NADPH and instead produces H_2O_2 , resulting in an ATP:NADPH demand of 1.57 (Fig. 4).

Overall, most of the APs cause relatively minor changes in the ATP:NADPH demand compared to native photorespiration with the notable exception of the complete decarboxylation Maier/South AP2 and South AP3 pathways, which cause large increases in the ATP:NADPH demand (Fig. 4).

Complete decarboxylation pathways require an increased rubisco carboxylation rate to have a benefit

Analysis so far has focused purely on photosynthetic energy efficiency and assumed no limitation of CO_2 diffusion either from outside the cell or between subcellular compartments. However, CO_2 diffusion poses a major limitation to photosynthesis in C3 plants (31). The complete decarboxylation pathways decrease the photosynthetic energy efficiency relative to WT photorespiration if unlimited CO_2 diffusion is assumed. However, if CO_2 diffusion into the chloroplast is limited, releasing CO_2 specifically within the chloroplast and thereby increasing the carboxylation rate relative to the oxygenation rate could be beneficial. We therefore determined the increase in carboxylation rate relative to the oxygenation rate necessary to compensate for the increased energy cost of the complete decarboxylation pathways.

To model the effect of an increased chloroplast CO_2 concentration, we constrained the rubisco carboxylase:oxygenase ratio of rubisco to a

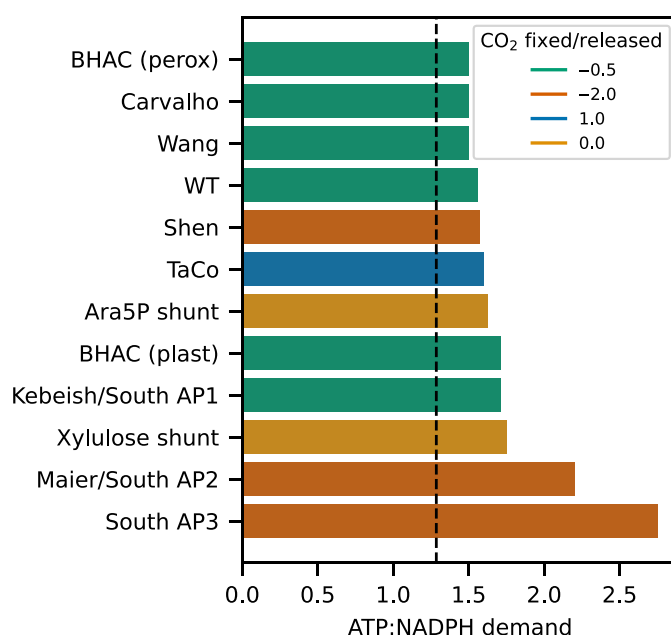


Fig. 4. Alternative pathways (APs) alter the ATP:NADPH demand of carbon fixation. The net ATP:NADPH demand of carbon fixation to GAP in the presence of APs calculated using the stoichiometric model and flux balance analysis (FBA) and assuming a rubisco carboxylase:oxygenase activity of 3:1. The dashed line represents the ATP:NADPH supplied by linear electron flow through the photosystems (9/7).

range of values and calculated the photosynthetic energy efficiency relative to the WT in terms of CO_2 fixed per photon absorbed. At a rubisco carboxylase:oxygenase ratio of 3:1, the complete decarboxylation pathways were less energetically efficient than WT photorespiration (Fig. 5). However, these pathways can become more energetically efficient than WT photorespiration if they are able to increase the chloroplast CO_2 concentration such that the rubisco carboxylase:oxygenase ratio reaches 4.8 to 6.1:1 (Fig. 5). This represents a 60 to 103% increase relative to the rubisco carboxylase:oxygenase ratio of 3:1 assumed for native photorespiration. The remaining partial decarboxylation, carbon-neutral, or carbon-fixing APs continue to show an increased photosynthetic efficiency relative to native photorespiration, even at lower rubisco carboxylase:oxygenase ratios (Fig. 5).

Native CO_2 refixation capacity affects AP benefit

Another factor that needs to be taken into account is that in native photorespiration, CO_2 released by glycine decarboxylase activity in the mitochondria can diffuse out of the cell before it reaches the chloroplast and is therefore only partly refixed. Plants have evolved mechanisms to recapture this CO_2 that would otherwise be lost, such as placing chloroplasts around the cell periphery (27, 32–35) or relocating the decarboxylation step to the bundle sheath cells, as in C3-C4 intermediate photosynthesis (36, 37). The exact amount of CO_2 refixation depends on both the plant species and environmental conditions (32, 37). APs can relocate the site of CO_2 release from the mitochondrion to the chloroplast and therefore potentially increase the proportion of refixed CO_2 .

CO_2 diffusion is dependent on a series of resistances between the external and internal airspace and between subcellular organelles (27, 33–35). These resistances were simplified in our stoichiometric model to a constraint on the fraction of CO_2 released in mitochondria

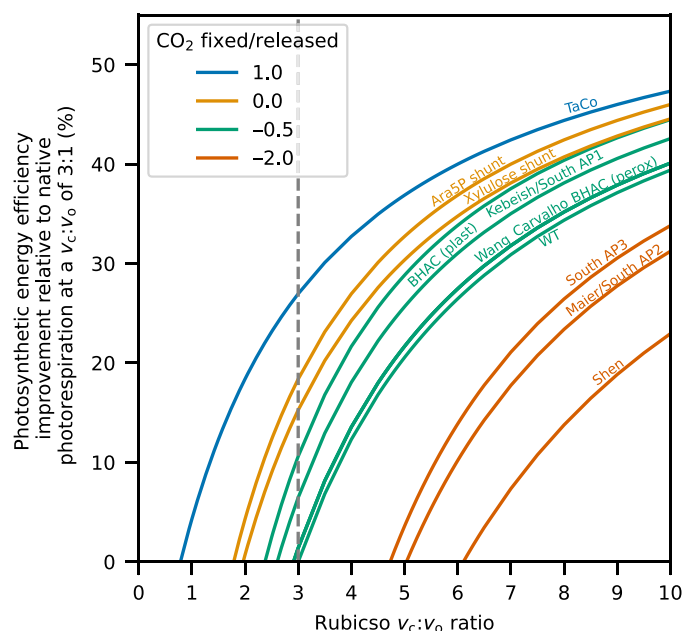


Fig. 5. Complete decarboxylation pathways require an increased rubisco carboxylase:oxygenase ratio to achieve an increased photosynthetic energy efficiency relative to wild-type (WT) photorespiration. Effect of altered rubisco carboxylase:oxygenase ($v_c:v_o$) ratio on photosynthetic energy efficiency of alternative pathways (APs) relative to WT photorespiration at a fixed rubisco carboxylase:oxygenase ratio of 3:1 (dashed gray line). Simulations were performed using the stoichiometric model and FBA with the objective set to maximization of GAP production. Photosynthetic energy efficiency was defined as the CO_2 fixed per photon absorbed.

that can be refixed by chloroplasts (refixation potential), with the remainder assumed to exit the leaf. We modeled the effect of different CO_2 refixation potentials in the WT plant on the relative carbon export of plants expressing APs compared to the WT. We assumed that relocation of CO_2 release by the APs to the chloroplast results in complete recapture of CO_2 released by the APs, therefore representing the maximum potential benefit. The input of CO_2 from outside the cell was fixed to the WT value to represent a CO_2 diffusion-limited condition and prevent cells from compensating for CO_2 lost from photorespiration or APs by simply importing more CO_2 . Photon input was constrained to the WT value representing an energy-limited condition, and the optimization objective was set to maximization of GAP production. In general, as the CO_2 refixation potential of the WT plant increases, the benefit of an AP that recaptures this otherwise lost CO_2 decreases (Fig. 6A). The maximum carbon export increase of any AP that recaptures otherwise lost CO_2 is 20% for a rubisco carboxylase:oxygenase ratio of 3:1 (Fig. 6A). Under the energy-limited condition modeled here, the APs that are more energetically efficient than native photorespiration (carbon-fixing, carbon-neutral, and partial decarboxylation pathways) can all achieve this maximum 20% benefit (Fig. 6A, all other APs). In contrast, the complete decarboxylation pathways, which are less energy efficient than native photorespiration, fixed less CO_2 than the WT plant at all CO_2 refixation potentials (Fig. 6A, dashed orange lines).

Next, we evaluated whether residual flux through the native photorespiratory pathway could be beneficial in combination with an AP. Native photorespiration potentially loses CO_2 from the cell

by releasing it in the mitochondria, affecting the carbon export. APs can recapture this CO_2 by releasing it in the chloroplast but can be more energetically expensive. Therefore, for the complete decarboxylation APs, there is a trade-off between the relatively more energy-efficient native photorespiration and the more carbon-efficient AP. We therefore repeated the previous analysis but allowed unlimited flux through native photorespiration and identified the optimal flux through native photorespiration and the AP under a CO_2 and energy limitation.

Under these energy- and CO_2 -limited conditions, the optimal flux distribution for the more energy-efficient pathways required zero flux through photorespiration (Fig. 6B). In contrast, for the less energy-efficient complete decarboxylation pathways, the optimal amount of native photorespiratory flux varied with the CO_2 refixation potential (Fig. 6B). In other words, residual flux through native photorespiration can compensate for the energy inefficiency of complete decarboxylation pathways, while the APs act to recapture otherwise lost CO_2 . Therefore, some residual photorespiratory flux can be beneficial in the presence of complete decarboxylation pathways, particularly when the CO_2 refixation potential is low (Fig. 6A, solid orange lines). The optimal flux through native photorespiration in combination with an AP may vary dynamically with the environmental conditions, which can affect CO_2 diffusion and the refixation potential of the plant. Overall, assuming that ~25% of CO_2 is refixed in a WT plant, all AP designs are advantageous when both CO_2 and energy are limiting and when operating in combination with native photorespiration (Fig. 6A, solid lines).

Understanding CO_2 dynamics requires kinetic modeling

Stoichiometric modeling demonstrated the energetic and stoichiometric benefits of the AP designs, how flux through certain APs can support amino acid biosynthesis, and the potential beneficial effects of avoiding CO_2 release in the mitochondria. However, the stoichiometric model required fixing the rubisco carboxylase:oxygenase ratio, whereas in vivo, it depends on the concentrations of O_2 and CO_2 , which can vary dynamically. Therefore, to model the effect of varying CO_2 diffusion and CO_2 concentration more accurately, we developed a kinetic model of photosynthesis to test the different AP designs.

The kinetic model was developed as a system of ordinary differential equations by combining models of the CBB cycle (38) and photorespiration (39), as well as a complete description of rubisco kinetics including carboxylation and oxygenation reactions (40). CO_2 was modeled as a dynamic variable to capture the effect of the various APs on the CO_2 concentration in the chloroplast. A fixed proportion (25%) of CO_2 released by glycine decarboxylase in the mitochondria was assumed to diffuse back into the chloroplast (32). The APs were implemented on top of this WT model and are grouped by their CO_2 stoichiometry, with the best-performing variant of each group shown in the following results. For a complete description of the model as well as a comparative analysis of intermediate model stages, see section S2.

Carbon-fixing pathways are more efficient at exporting carbons

We first evaluated the different AP designs under reference conditions of 400-parts per million atmospheric CO_2 and an illumination of $700 \mu\text{mol}/\text{m}^2 \text{ s}$. From this analysis, we calculated the rubisco carboxylation and oxygenation rates (v_c and v_o , respectively) and rubisco carboxylase:oxygenase ratio. We further extended the

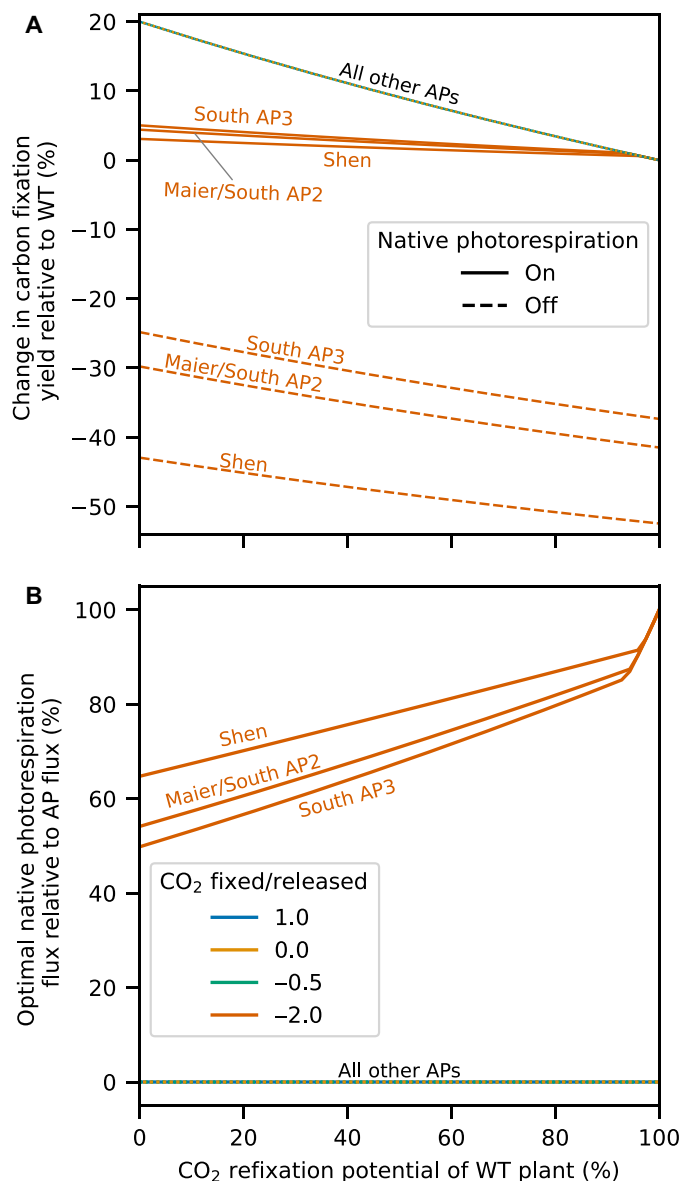


Fig. 6. The benefit of an alternative pathway (AP) that recaptures otherwise lost CO₂ depends on how effective the wild-type (WT) plant is at already re-fixing CO₂ released by photorespiration. (A) Effect of CO₂ refixation in WT plants on the relative benefit of APs to carbon fixation calculated using the stoichiometric model and flux balance analysis (FBA). Refixation potential is defined as the fraction of CO₂ released from photorespiration in the mitochondria that could enter the chloroplast rather than leaving the cell. The refixation potential of a WT cell was fixed between 0 and 100%, and the objective was set to maximization of GAP production. Rubisco carboxylase:oxygenase activity was constrained to 3:1. When simulating the APs, photon and CO₂ inputs were constrained to the WT value required to generate GAP at a rate of 1 $\mu\text{mol s}^{-1}$ representing an energy- and CO₂-limited condition. Dashed lines are with flux through native photorespiration blocked; solid lines are with native photorespiration free to carry flux. (B) Optimal flux through native photorespiration relative to the AP at varying CO₂ refixation potentials. Photon and CO₂ inputs were constrained as in (A). 100% means that there is no flux through the AP, and 0% means that the AP completely replaces photorespiration.

evaluation by considering export of triose-phosphates and hexoses as a proxy for plant growth and defined the carbon-use efficiency as the ratio of carbon export rate relative to the rubisco carboxylase rate.

The carbon-fixing pathways show a reduced rubisco carboxylation rate (less than 60% of the WT) and slightly increased oxygenation rate, leading to a reduced rubisco carboxylase:oxygenase ratio relative to the WT (Fig. 7). The complete decarboxylation APs show the exact opposite, with a higher carboxylation rate (more than 125% of the WT) and lower oxygenation rate, leading to a rubisco carboxylase:oxygenase ratio of more than 175% relative to the WT (Fig. 7). Even if the secondary carboxylation steps like glycolyl-CoA carboxylase in the carbon-fixing TaCo pathway are counted in the total carboxylation rate, this general trend stays the same, even though, now, the total carbon fixation of the carbon-fixing APs is less decreased than the carbon-neutral pathways (Fig. 7, transparent area). Contrastingly, the carbon export is the highest for the carbon-fixing APs (around 120%) and the lowest for the complete decarboxylation APs at slightly above 100% (Fig. 7). This is reflected by the carbon-use efficiency, which is the highest for the carbon-fixing APs at around 190% and the lowest for the complete decarboxylation APs at around 80% (Fig. 7). This increase in carbon-use efficiency in carbon-neutral and carbon-fixing APs is caused by the fact that they generate intermediates, other than CO₂, that can enter the CBB cycle. By increasing the input of intermediates into the cycle, more carbon can be withdrawn without requiring additional fixation of CO₂ by rubisco. Therefore, carbon-fixing and carbon-neutral alternative photorespiratory pathways increase the carbon-use efficiency of the CBB cycle, resulting in more carbon exported per rubisco carboxylase reaction.

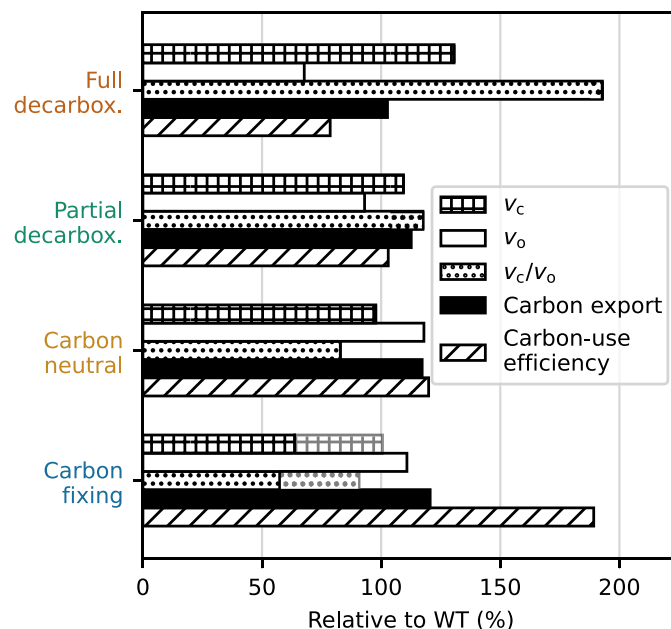


Fig. 7. Steady-state performance indicators of plant metabolism simulated by the kinetic model for different alternative pathway (AP) designs, grouped by their CO₂ stoichiometry. The simulation was performed under reference conditions of 400-parts per million atmospheric CO₂ and an illumination of 700 $\mu\text{mol/m}^2$ s. Transparent bars signify the addition of secondary carboxylation steps to the measurement of rubisco carboxylation rate for the carbon-fixing pathways. The different AP designs are grouped by their CO₂ stoichiometry, and only the pathway variant with the maximal carbon export of the group is shown.

APs are most beneficial at low intracellular CO₂

The activity and effectiveness of the APs, which we measure as the improvement of carbon export, depend on the local CO₂ concentration in the chloroplast. The velocity at which this local CO₂ can be replenished is dependent on the external CO₂ concentration as well as the internal transport rate. We systematically evaluated all AP designs for both of these factors. The improvement of carbon export relative to the WT is the highest for both low CO₂-transport rate (Fig. 8D) and low external CO₂ concentration (fig. S1), in which the carbon-fixing pathways perform best (Fig. 8D). These are also the conditions where the absolute rates of carbon export are reduced

(Fig. 8B). The carbon-fixing APs consistently show the highest improvement relative to the WT, closely followed by the carbon-neutral APs and then by the partial decarboxylation APs (Fig. 8D). The full decarboxylation APs show the lowest improvement and perform worse than the WT if the CO₂-transport rate is increased more than 10% (Fig. 8D). The improvement to carbon export diminishes for all APs under very high CO₂ conditions (fig. S1).

High light increases AP benefit

All APs require more energy equivalents than the CBB cycle per carbon export and the full decarboxylation pathways even more than

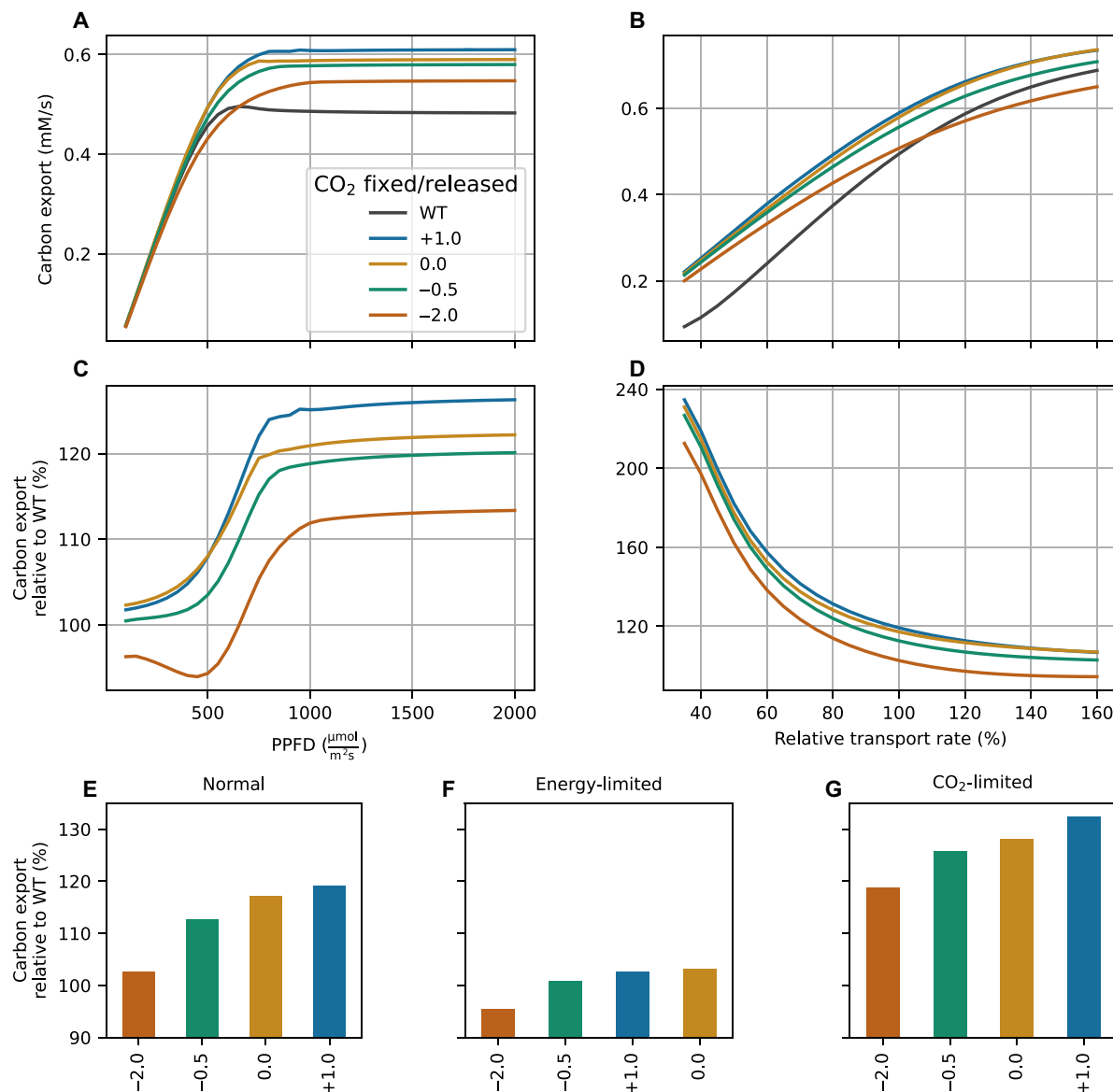


Fig. 8. Steady-state carbon export of alternative pathways (APs) simulated by the kinetic model depending on photosynthetic photon flux density (PPFD) or CO₂ transport rate. Carbon export is shown in both absolute terms (A and B) and relative to the wild-type (WT) under the same conditions (C and D). Three representative scenarios are highlighted for a well-watered plant in a temperate climate with sufficient light (700 $\mu\text{mol}/\text{m}^2/\text{s}$) (E); a well-watered plant in temperate climate with low light (250 $\mu\text{mol}/\text{m}^2/\text{s}$), which is thus energy limited (F); and a hot and dry climate with low water supply and, thus, partially closed stomata (90% of WT CO₂ transport rate), which is thus CO₂ limited (G). The different AP designs are grouped by their CO₂ stoichiometry (−2, −0.5, 0, and 1), and only the pathway variant with the maximal carbon export of the group is shown.

native photorespiration. Therefore, it is important to assess how much energy supply is necessary such that the benefits of the pathways outweigh this energy cost. As natural light conditions can be continuously fluctuating, the AP performance should be assessed under a variety of light conditions. We did this by systematically scanning the effect of illumination on the carbon export, by simulating the steady state for each photosynthetic photon flux density (PPFD).

Here, we found that all APs show the highest increase in carbon export relative to native photorespiration under high-light conditions, with the carbon-fixing APs showing the highest increase in carbon export at 125% relative to the WT (Fig. 8C). The second-best option is carbon-neutral pathways, which, under low-light conditions, outperform the carbon-fixing pathways (Fig. 8C, illumination below 400 μmol). The complete decarboxylation pathways show a beneficial effect for medium- and high-light conditions compared to the WT but are disadvantageous under low-light conditions compared to the other APs (Fig. 8C). These results demonstrate that under medium- to high-light conditions, the benefits of all APs outweigh the increased direct energy cost, while at low light, the increased energy demand outweighs the benefits for the complete decarboxylation APs.

Environmental conditions require different AP designs

The previous results highlight that depending on the environmental conditions, which will affect CO_2 diffusion and light intensity, different APs should be used to maximize carbon export. We predicted the carbon export improvement of different APs for three distinct scenarios. The first one is a normal scenario, which corresponds to a well-watered plant in a temperate climate with sufficient light. The next one is a scenario with a well-watered plant in temperate climate but low light, which is thus energy limited. For this, we used an illumination of 250 $\mu\text{mol}/\text{m}^2 \text{ s}$. The last one is a scenario of a hot and dry climate and high light, with partially closed stomata, which is thus CO_2 limited. This is represented by lowering the carbon transport rate to 90% of the WT.

In both the normal and CO_2 -limited scenarios, the carbon-fixing APs show the highest carbon export (Fig. 8, E and G). Under energy-limiting conditions, carbon-fixing and carbon-neutral APs show similar carbon export (Fig. 8F). In all cases, complete decarboxylation pathways show the lowest carbon export, with a negative effect under energy-limited conditions, a slightly positive effect under normal conditions, and a positive effect under CO_2 -limited conditions (Fig. 8, E to G). Thus, in most scenarios, the carbon-fixing APs are the preferred choice, while under energy-limited conditions, the carbon-neutral APs might be more beneficial.

DISCUSSION

Using various mathematical models of plant metabolism, we have comprehensively identified and assessed the mechanisms by which APs can enhance carbon assimilation and growth. To understand how environmental conditions and plant physiology can affect pathway benefits, we also quantitatively assessed the effects of light intensity and CO_2 availability on the different APs. We show that carbon-fixing APs, such as the TaCo pathway, have the greatest potential benefit over a range of conditions and could provide an increase in carbon export from photosynthesis of more than 20%. Because of the initial exponential growth phase of plants, such a percentage could generate substantial gains in biomass over time (41).

APs use distinct mechanisms to improve growth

Our work showed that APs to photorespiration can provide benefits to plants via five different mechanisms (Fig. 9): (i) an energy efficiency benefit by metabolizing the 2PG produced by the rubisco oxygenase reaction in a way that uses less ATP and reducing power compared to native photorespiration; (ii) a biosynthetic energy efficiency benefit if intermediates of the AP can be used for biosynthetic reactions; (iii) recapture of CO_2 that could otherwise diffuse from the cell; (iv) an increased CO_2 concentration at the site of rubisco in the chloroplasts caused by altered CO_2 diffusion within the cell; and (v) increased carbon-use efficiency of the CBB cycle caused by an additional input of CBB cycle intermediates, which enables more carbon to be exported per rubisco carboxylase reaction. As CO_2 diffusion differs depending on cell morphology and leaf physiology, these CO_2 -related benefits can be different in different plant species. Thus, next to simply clearing the 2PG produced by the rubisco oxygenase reaction, alternative photorespiratory pathways can have broad effects on the plant in terms of energetics, biosynthesis, and CO_2 dynamics and these must be considered at the system level to evaluate the effectiveness of any pathway.

Benefits of APs depend on environmental conditions

The environmental conditions a plant grows in, such as light intensity, temperature, and water availability, can affect the benefit of the different mechanisms that APs use. Under low-light conditions, when energy is limiting, the energy efficiency of APs becomes critical to their effectiveness (10, 42). Our models showed that APs that are more energy efficient than native photorespiration will offer greater benefits in low light, which is experimentally supported by growth enhancement in *Arabidopsis* expressing the Kebeish pathway and grown under low-light and short-day conditions (14). In contrast, complete decarboxylation pathways, which are less energy efficient than native photorespiration, are predicted to show no benefits under these low-light conditions. Under high-light conditions, energy efficiency no longer offers an advantage, and the pathways' effects on CO_2 diffusion and fixation become more important. Our analyses predict all pathways to perform best under high-light conditions (Fig. 8, A and C), suggesting that benefits from altered CO_2 diffusion have the biggest potential to increase plant growth. This finding is also supported experimentally with complete decarboxylation pathways including South AP3, Shen, and Wang all showing increased benefits under high-light conditions (5, 15, 20). Overall, the APs provide the greatest benefit over native photorespiration under high-light and CO_2 -limiting conditions, with certain pathways also able to provide benefits under low-light conditions.

The benefits of APs are comparable to those predicted for C3-C4 intermediate or C4 metabolism (43). The conditions that favor these naturally evolved mechanisms are also those we identified as beneficial for the APs. However, from a metabolic engineering perspective, the APs described here offer advantages over introducing C3-C4 or C4 metabolism into a C3 plant, as they can require as few as three genes compared to the >15 genetic modifications potentially needed to support the biochemistry, leaf anatomy, and intercellular transport of C3-C4 or C4 photosynthesis. Therefore, APs offer a more easily implementable solution to the same problems that C3-C4 intermediate and C4 photosynthesis has evolved to address.

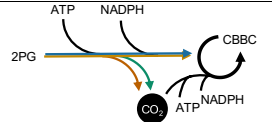
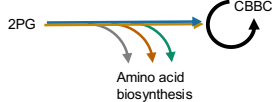
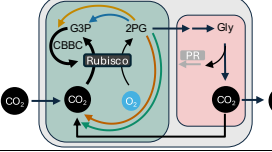
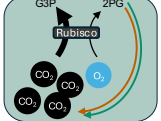
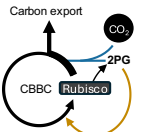
Direct or indirect effect of pathway		Pathway effect applies to carbon stoichiometry				Interactions with physiology and environment
		-2	-0.5	0	1	
i) Energy efficiency			●	●	●	Most relevant when energy is limiting, i.e., low light
ii) Biosynthetic efficiency		●	●*			Depends on biomass composition and if leaves are growing or mature
iii) CO2 recapture		●	●†	●	●	Depends on mitochondria/chloroplast arrangement, leaf CO2 diffusion, chloroplast CO2 permeability
iv) Increase chloroplast CO2 concentration		●	●†			Depends on chloroplast CO2 permeability
v) Increase CBB cycle carbon use efficiency				●	●	High-light and low-CO2 scenarios provide the greatest relative increase in carbon export

Fig. 9. Alternative photorespiratory pathways can affect carbon assimilation and growth in multiple ways. Asterisk (*): only applies to BHAC and Carvalho pathways, not Wang and Kebeish/South AP1 pathways, which do not generate biosynthetic intermediates. Dagger symbol (†): Only applies to pathways that relocate CO₂ release to chloroplasts, i.e., not Carvalho or BHAC (perox) pathways, which are peroxisomal. G3P, glyceraldehyde-3-phosphate.

Applying insights to previous results

By applying the insight we have gained, we can now try to better explain previous experimental observations. For example, complete decarboxylation pathways such as the Maier/South AP2, South AP3, and Shen bypasses experimentally showed growth benefits, but the molecular basis for these benefits was less clear, as previous computational analysis based on a kinetic model describing carbon fixation and subcellular CO₂ conductance did not predict an enhanced rate of photosynthesis (10). Here, we quantitatively demonstrate that complete decarboxylation pathways can enhance photosynthesis by increasing the CO₂ concentration in the chloroplast and, subsequently, the rubisco carboxylase:oxygenase ratio, as well as by recapturing otherwise lost CO₂. These effects are consistent with experimental measurements of unchanged or decreased CO₂ compensation points in engineered plants expressing these pathways (15, 19, 20, 44). Furthermore, for complete decarboxylation and some partial decarboxylation pathways, we demonstrated additional increases in energy efficiency in cells synthesizing amino acids for biomass synthesis or phloem exudate that has not previously been identified. Thus, through our work, we can now better explain the reasons why, in previous studies, a particular AP has generated benefits.

Some aspects of APs require future investigation

Yet, despite improving our understanding of alternative photorespiratory pathways, a number of experimental observations remain

unexplained. For example, the South AP3 pathway expressed in tobacco shows increased CO₂ assimilation even at very high intracellular CO₂ (15). Decarboxylation pathways reduce rubisco oxygenase activity by increasing the local CO₂ concentration at increased energetic costs. At very high intracellular CO₂, this mechanism cannot offer any additional benefit, as the CO₂ concentration in the chloroplast should already be high. The mechanism of the benefit of the South AP3 pathway even at high CO₂ remains unexplained and may relate to the reported beneficial effects of expressing glycolate dehydrogenase alone, which could affect the efficiency of photosynthetic electron transport (14, 45–47). In addition, our models predicted that partial decarboxylation pathways should outperform full decarboxylation pathways across conditions. However, comparison of the partial decarboxylation South AP1 and the complete decarboxylation South AP3 expressed in tobacco in greenhouse trials showed greater yield increases in the AP3 pathway (15). In this context, it is important to realize that our model predictions reflect best-case scenarios, requiring optimal expression and kinetics of the pathway enzymes. While a discrepancy between our model predictions and experimental implementations of APs could point to shortcomings in our models, an alternative explanation for the discrepancy could be that an engineered plant might not yet have optimal enzyme expression levels. Thus, such a discrepancy might also indicate potential for further improvements of plant performance.

Outlook

With this work, we have improved our mechanistic understanding of how alternative photorespiratory pathways can enhance carbon assimilation and growth and used this to predict that the carbon-fixing TaCo pathway represents the best option for increasing crop yields over a range of conditions. In the future, crops, or specific cultivars, should be screened to identify those with limitations in CO₂ refixation capacity or CO₂ diffusion that make them most likely to benefit from engineering with APs to native photorespiration. The models presented here could also be used to evaluate or develop new AP designs that may further increase yield gains, e.g., by targeting specific growth scenarios, such as the juvenile or adult growth stages, or specific crop species. With the ability to more rationally engineer alternative photorespiratory pathways into suitable crops and identify their optimal growing conditions, our work will hopefully contribute to realizing the maximum impact of alternative photorespiratory pathways for improving crop yields.

MATERIALS AND METHODS

Stoichiometric model

A stoichiometric model of core plant metabolism based on an *Arabidopsis* leaf, PlantCoreMetabolism_v3, was curated starting from a previously described model [PlantCoreMetabolism_v1_2; (22)]. The model is available in SBML format as an XML file in (48) and <https://gitlab.com/gain4crops/2024-paper>. Python 3, COBRApy (49), and the CPLEX solver were used for flux balance analysis (FBA) optimizations. Output fluxes to phloem exudate were defined from *Arabidopsis* phloem composition (29). Output fluxes to biomass were defined as described in the AraGEM model (30). Net ATP demands were calculated by quantifying the flux through both plastidic and mitochondrial ATP synthases. As the model is autotrophic, all ATP must ultimately be generated by either plastidic ATP synthase or by mitochondrial ATP synthase using NADH generated in the plastid. To calculate the reductant demand, the flux through proton pumping mitochondrial NADH-dehydrogenase (which is used for generating ATP) was subtracted from the flux through plastidic ferredoxin-NADP reductase. All codes required to reproduce the results are available in (48) and at <https://gitlab.com/gain4crops/2024-paper> as Jupyter notebook files.

Kinetic model

The ordinary differential equation model was built mainly using two previously published models of the CBB cycle (38, 50) and photorespiration (39) and developed using Python-based software modelbase (51). Rubisco kinetics including carboxylation and oxygenation reactions were described on the basis of the rate equation from Witzel *et al.* (40). Energy metabolites, ATP, and NADPH were implemented as dynamic variables as in (52), and their production was modeled using a simplified light-dependent reaction with an additional quenching reaction to account for the different ATP and NADPH demands of the system. Thioredoxin-based redox regulation of CBB cycle enzymes was linked to the energy status of the model via an NADPH thioredoxin reductase reaction based on the description by Saadat *et al.* (53). CO₂ was modeled dynamically with CO₂ input from the atmosphere described with a diffusion equation. As refixation of respired and photorespired CO₂ was shown to range between 24 and 38% in wheat and rice (32), a static CO₂ refixation of 25% from mitochondrial glycine decarboxylation was

assumed with the remaining CO₂ lost to the atmosphere. For APs that relocate CO₂ to the chloroplast, we assumed that 100% of this could potentially be refixed. Ammonia was also modeled as a dynamic variable along with ammonium assimilation into glutamate and the associated energy costs. The model was built in a stepwise manner, with each iteration being compared to the previous one to ensure that the changes made were valid (see section S2 for a complete description). The final model was used as a reference point, called WT, and the APs were implemented on top of this model. Native photorespiration was deactivated in the presence of the APs by setting the V_{\max} of the first native photorespiratory enzyme that was not used by the respective AP to zero. The AP designs were grouped by their CO₂ stoichiometry, and the best-performing pathway of each group is shown in the Results. All codes required to reproduce the results are available in (48) and at <https://gitlab.com/gain4crops/2024-paper>.

Supplementary Materials

This PDF file includes:

Supplementary Text

Figs. S1 to S18

Tables S1 to S38

References

REFERENCES AND NOTES

1. T. D. Sharkey, Estimating the rate of photorespiration in leaves. *Physiol. Plant.* **73**, 147–152 (1988).
2. B. J. Walker, A. Vanlooche, C. J. Bernacchi, D. R. Ort, The costs of photorespiration to food production now and in the future. *Annu. Rev. Plant Biol.* **67**, 107–129 (2016).
3. M. Betti, H. Bauwe, F. A. Busch, A. R. Fernie, O. Keech, M. Levey, D. R. Ort, M. A. J. Parry, R. Sage, S. Timm, B. Walker, A. P. M. Weber, Manipulating photorespiration to increase plant productivity: Recent advances and perspectives for crop improvement. *J. Exp. Bot.* **67**, 2977–2988 (2016).
4. E. N. Smith, M. van Aalst, T. Tosens, Ü. Niinemets, B. Stich, T. Morosinotto, A. Alboresi, T. Erb, P. A. Gómez-Coronado, D. Tolleter, G. Finazzi, G. Curien, M. Heinemann, O. Ebenhöf, J. M. Hibberd, U. Schlüter, T. Sun, A. P. M. Weber, Improving photosynthetic efficiency toward food security: Strategies, advances, and perspectives. *Mol. Plant* **16**, 1547–1563 (2023).
5. L.-M. Wang, B.-R. Shen, B.-D. Li, C.-L. Zhang, M. Lin, P.-P. Tong, L.-L. Cui, Z.-S. Zhang, X.-X. Peng, A synthetic photorespiratory shortcut enhances photosynthesis to boost biomass and grain yield in rice. *Mol. Plant* **13**, 1802–1815 (2020).
6. D. D. Strand, B. J. Walker, Energetic considerations for engineering novel biochemistries in photosynthetic organisms. *Front. Plant Sci.* **14**, 1116812 (2023).
7. S. Rachmilevitch, A. B. Cousins, A. J. Bloom, Nitrate assimilation in plant shoots depends on photorespiration. *Proc. Natl. Acad. Sci. U.S.A.* **101**, 11506–11510 (2004).
8. R. Li, M. Moore, J. King, Investigating the regulation of one-carbon metabolism in *Arabidopsis thaliana*. *Plant Cell Physiol.* **44**, 233–241 (2003).
9. X. Fu, L. M. Gregory, S. E. Weise, B. J. Walker, Integrated flux and pool size analysis in plant central metabolism reveals unique roles of glycine and serine during photorespiration. *Nat. Plants* **9**, 169–178 (2023).
10. C.-P. Xin, D. Tholen, V. Devloo, X.-G. Zhu, The benefits of photorespiratory bypasses: How can they work? *Plant Physiol.* **167**, 574–585 (2015).
11. D. L. Trudeau, C. Edlich-Muth, J. Zarzycki, M. Scheffen, M. Goldsmith, O. Khersonsky, Z. Avizemer, S. J. Fleishman, C. A. R. Cotton, T. J. Erb, D. S. Tawfik, A. Bar-Even, Design and in vitro realization of carbon-conserving photorespiration. *Proc. Natl. Acad. Sci. U.S.A.* **115**, E11455–E11464 (2018).
12. M. Scheffen, D. G. Marchal, T. Beneyton, S. K. Schuller, M. Klose, C. Diehl, J. Lehmann, P. Pfister, M. Carrillo, H. He, S. Aslan, N. S. Cortina, P. Claus, D. Bollschweiler, J. C. Baret, J. M. Schuller, J. Zarzycki, A. Bar-Even, T. J. Erb, A new-to-nature carboxylation module to improve natural and synthetic CO₂ fixation. *Nat. Catal.* **4**, 105–115 (2021).
13. D. G. Marchal, L. Schulz, I. Schuster, J. Ivanovska, N. Paczia, S. Prinz, J. Zarzycki, T. J. Erb, Machine learning-supported enzyme engineering toward improved CO₂-fixation of glycolyl-CoA carboxylase. *ACS Synth. Biol.* **12**, 3521–3530 (2023).
14. R. Kebeish, M. Niessen, K. Thiruveedhi, R. Bari, H.-J. Hirsch, R. Rosenkranz, N. Stäbler, B. Schönfeld, F. Kreuzaler, C. Peterhänsel, Chloroplastic photorespiratory bypass increases photosynthesis and biomass production in *Arabidopsis thaliana*. *Nat. Biotechnol.* **25**, 593–599 (2007).

15. P. F. South, A. P. Cavanagh, H. W. Liu, D. R. Ort, Synthetic glycolate metabolism pathways stimulate crop growth and productivity in the field. *Science* **363**, eaat9077 (2019).
16. J. de F. C. Carvalho, P. J. Madgwick, S. J. Powers, A. J. Keys, P. J. Lea, M. A. J. Parry, An engineered pathway for glyoxylate metabolism in tobacco plants aimed to avoid the release of ammonia in photorespiration. *BMC Biotechnol.* **11**, 1–17 (2011).
17. M.-S. Roell, L. S. von Borzykowski, P. Westhoff, A. Plett, N. Paczia, P. Claus, S. Urte, T. J. Erb, A. P. M. Weber, A synthetic C4 shuttle via the β -hydroxyaspartate cycle in C3 plants. *Proc. Natl. Acad. Sci. U.S.A.* **118**, e2022307118 (2021).
18. L. S. von Borzykowski, F. Severi, K. Krüger, L. Hermann, A. Gilardet, F. Sippel, B. Pommerenke, P. Claus, N. S. Cortina, T. Glatter, S. Zauner, J. Zarzycki, B. M. Fuchs, E. Bremer, U. G. Maier, R. I. Amann, T. J. Erb, Marine Proteobacteria metabolize glycolate via the β -hydroxyaspartate cycle. *Nature* **575**, 500–504 (2019).
19. A. Maier, H. Fahnenstich, S. von Caemmerer, M. K. M. Engqvist, A. P. M. Weber, U. I. Flügge, V. G. Maurino, Transgenic introduction of a glycolate oxidative cycle into A. Thaliana chloroplasts leads to growth improvement. *Front. Plant Sci.* **3**, 38 (2012).
20. B.-R. Shen, L.-M. Wang, X.-L. Lin, Z. Yao, H.-W. Xu, C.-H. Zhu, H.-Y. Teng, L.-L. Cui, E.-E. Liu, J.-J. Zhang, Z.-H. He, X.-X. Peng, Engineering a new chloroplastic photorespiratory bypass to increase photosynthetic efficiency and productivity in rice. *Mol. Plant* **12**, 199–214 (2019).
21. M. H. Aboelmy, C. Peterhansel, Enzymatic characterization of Chlamydomonas reinhardtii glycolate dehydrogenase and its nearest proteobacterial homologue. *Plant Physiol. Biochem.* **79**, 25–30 (2014).
22. S. Shameer, R. G. Ratcliffe, L. J. Sweetlove, Leaf energy balance requires mitochondrial respiration and export of chloroplast NADPH in the light. *Plant Physiol.* **180**, 1947–1961 (2019).
23. F. Ma, L. J. Jazmin, J. D. Young, D. K. Allen, Isotopically nonstationary ^{13}C flux analysis of changes in Arabidopsis thaliana leaf metabolism due to high light acclimation. *Proc. Natl. Acad. Sci. U.S.A.* **111**, 16967–16972 (2014).
24. K. R. Hanson, R. B. Peterson, The stoichiometry of photorespiration during C3-photosynthesis is not fixed: Evidence from combined physical and stereochemical methods. *Arch. Biochem. Biophys.* **237**, 300–313 (1985).
25. A. B. Cousins, I. Pracharoenwattana, W. Zhou, S. M. Smith, M. R. Badger, Peroxisomal malate dehydrogenase is not essential for photorespiration in Arabidopsis but its absence causes an increase in the stoichiometry of photorespiratory CO_2 release. *Plant Physiol.* **148**, 786–795 (2008).
26. A. B. Cousins, B. J. Walker, I. Pracharoenwattana, S. M. Smith, M. R. Badger, Peroxisomal hydroxypyruvate reductase is not essential for photorespiration in Arabidopsis but its absence causes an increase in the stoichiometry of photorespiratory CO_2 release. *Photosynth. Res.* **108**, 91–100 (2011).
27. F. A. Busch, Photorespiration in the context of Rubisco biochemistry, CO_2 diffusion and metabolism. *Plant J.* **101**, 919–939 (2020).
28. K. R. Hanson, R. B. Peterson, Regulation of photorespiration in leaves: Evidence that the fraction of ribulose biphosphate oxygenated is conserved and stoichiometry fluctuates. *Arch. Biochem. Biophys.* **246**, 332–346 (1986).
29. T. L. Wilkinson, A. E. Douglas, Phloem amino acids and the host plant range of the polyphagous aphid, *Aphis fabae*. *Entomol. Exp. Appl.* **106**, 103–113 (2003).
30. C. G. de Oliveira Dal'Molin, L.-E. Quek, P. A. Saa, L. K. Nielsen, A multi-tissue genome-scale metabolic modeling framework for the analysis of whole plant systems. *Front. Plant Sci.* **6**, 4 (2015).
31. J. R. Evans, R. Kaldenhoff, B. Genty, I. Terashima, Resistances along the CO_2 diffusion pathway inside leaves. *J. Exp. Bot.* **60**, 2235–2248 (2009).
32. F. A. Busch, T. L. Sage, A. B. Cousins, R. F. Sage, C3 plants enhance rates of photosynthesis by reassimilating photorespired and respired CO_2 . *Plant Cell Environ.* **36**, 200–212 (2013).
33. D. Tholen, G. Ethier, B. Genty, S. Pepin, X.-G. Zhu, Variable mesophyll conductance revisited: Theoretical background and experimental implications. *Plant Cell Environ.* **35**, 2087–2103 (2012).
34. D. Tholen, G. Ethier, B. Genty, Mesophyll conductance with a twist. *Plant Cell Environ.* **37**, 2456–2458 (2014).
35. X. Yin, P. C. Struik, Simple generalisation of a mesophyll resistance model for various intracellular arrangements of chloroplasts and mitochondria in C3 leaves. *Photosynth. Res.* **132**, 211–220 (2017).
36. U. Schlüter, J. W. Bouvier, R. Guerreiro, M. Malisic, C. Kontny, P. Westhoff, B. Stich, A. P. M. Weber, Brassicaceae display variation in efficiency of photorespiratory carbon-recapturing mechanisms. *J. Exp. Bot.* **74**, 6631–6649 (2023).
37. O. Keerberg, T. Pärnik, H. Ivanova, B. Bassüner, H. Bauwe, C2 photosynthesis generates about 3-fold elevated leaf CO_2 levels in the C3–C4 intermediate species *Flaveria pubescens*. *J. Exp. Bot.* **65**, 3649–3656 (2014).
38. M. G. Poolman, D. A. Fell, S. Thomas, Modelling photosynthesis and its control. *J. Exp. Bot.* **51**, 319–328 (2000).
39. A. Yokota, H. Komura, S. Kitaoka, Refixation of photorespired CO_2 during photosynthesis in *Euglena gracilis* z. *Agric. Biol. Chem.* **49**, 3309–3310 (1985).
40. F. Witzel, J. Götze, O. Ebenhöf, Slow deactivation of ribulose 1, 5-bisphosphate carboxylase/oxygenase elucidated by mathematical models. *FEBS J.* **277**, 931–950 (2010).
41. M. U. F. Kirschbaum, Does enhanced photosynthesis enhance growth? Lessons learned from CO_2 enrichment studies. *Plant Physiol.* **155**, 117–124 (2011).
42. C. Peterhansel, C. Blume, S. Offermann, Photorespiratory bypasses: How can they work? *J. Exp. Bot.* **64**, 709–715 (2013).
43. C. Bellasio, G. D. Farquhar, A leaf-level biochemical model simulating the introduction of C2 and C4 photosynthesis in C3 rice: Gains, losses and metabolite fluxes. *New Phytol.* **223**, 150–166 (2019).
44. A. P. Cavanagh, P. F. South, C. J. Bernacchi, D. R. Ort, Alternative pathway to photorespiration protects growth and productivity at elevated temperatures in a model crop. *Plant Biotechnol. J.* **20**, 711–721 (2022).
45. G. Nölke, M. Houdelet, F. Kreuzaler, C. Peterhansel, S. Schillberg, The expression of a recombinant glycolate dehydrogenase polypeptide in potato (*Solanum tuberosum*) plastids strongly enhances photosynthesis and tuber yield. *Plant Biotechnol. J.* **12**, 734–742 (2014).
46. J. Dalal, H. Lopez, N. B. Vasani, Z. Hu, J. E. Swift, R. Yalamanchili, M. Dvora, X. Lin, D. Xie, R. Qu, H. W. Sederoff, A photorespiratory bypass increases plant growth and seed yield in biofuel crop *Camelina sativa*. *Biotechnol. Biofuels* **8**, 175 (2015).
47. A. Z. Abbasi, M. Bilal, G. Khurshid, C. Yiotis, I. Zeb, J. Hussain, A. Baig, M. M. Shah, S. U. Chaudhary, B. Osborne, R. Ahmad, Expression of cyanobacterial genes enhanced CO_2 assimilation and biomass production in transgenic *Arabidopsis thaliana*. *PeerJ* **9**, e11860–e11833 (2021).
48. E. N. Smith, M. Van Aalst, A. P. M. Weber, O. Ebenhöf, M. Heinemann. Code accompanying “Alternatives to photorespiration: A systems-level analysis reveals mechanisms of enhanced plant productivity” version 1, Zenodo (2025); <https://doi.org/10.5281/zenodo.14628439>.
49. A. Ebrahim, J. A. Lerman, B. O. Palsson, D. R. Hyduke, COBRApy: Constraints-Based Reconstruction and Analysis for Python. *BMC Syst. Biol.* **7**, 74 (2013).
50. G. Pettersson, U. Ryde-Pettersson, A mathematical model of the Calvin photosynthesis cycle. *Eur. J. Biochem.* **175**, 661–672 (1988).
51. M. van Aalst, O. Ebenhöf, A. Matuszyńska, Constructing and analysing dynamic models with modelbase v1. 2.3: A software update. *BMC Bioinf.* **22**, 203 (2021).
52. A. Matuszyńska, N. P. Saadat, O. Ebenhöf, Balancing energy supply during photosynthesis – A theoretical perspective. *Physiol. Plant.* **166**, 392–402 (2019).
53. N. P. Saadat, T. Nies, M. Van Aalst, B. Hank, B. Demirtas, O. Ebenhöf, A. Matuszyńska, Computational analysis of alternative photosynthetic electron flows linked with oxidative stress. *Front. Plant Sci.* **12**, 750580 (2021).
54. M. E. Beber, M. G. Gollub, D. Mozaffari, K. M. Shebek, A. I. Flamholz, R. Milo, E. Noor, EQuilibrator 3.0: A database solution for thermodynamic constant estimation. *Nucleic Acids Res.* **50**, D603–D609 (2022).

Acknowledgments

Funding: This work was supported by the following: European Union H2020 Program project GAIN4CROPS, grant agreement no. 862087 (to E.N.S., M.v.A., O.E., A.P.M.W., and M.H.); Deutsche Forschungsgemeinschaft Cluster of Excellence for Plant Sciences (CEPLAS); and Germany's Excellence Strategy EXC-2048/1, project ID 390686111 (to O.E. and A.P.M.W.). **Author contributions:** Conceptualization: O.E., A.P.M.W., E.N.S., M.H., and M.v.A. Data curation: M.v.A. and E.N.S. Formal analysis: O.E., M.v.A., and E.N.S. Funding acquisition: A.P.M.W., O.E., and M.H. Investigation: E.N.S. and M.v.A. Methodology: O.E., M.v.A., and E.N.S. Project administration: A.P.M.W., M.H., and O.E. Resources: O.E., M.H., M.v.A., and E.N.S. Software: M.v.A. and E.N.S. Supervision: M.H. and O.E. Validation: O.E., M.v.A., and E.N.S. Visualization: M.v.A. and E.N.S. Writing—original draft: E.N.S., M.H., and M.v.A. Writing—review and editing: O.E., A.P.M.W., M.H., and E.N.S. **Competing interests:** A.P.M.W. is an inventor on a pending patent related to this work filed by the Heinrich Heine University (no. WO2021023801A filed 8 May 2020, published 2 November 2021). The other authors declare that they have no competing interests. **Data and materials availability:** All codes required to reproduce the results are available on Zenodo (48), or the latest version can be found at <https://gitlab.com/gain4crops/2024-paper>. All other data needed to evaluate the conclusions in this paper are present in the paper and/or the Supplementary Materials.

Submitted 18 October 2024

Accepted 25 February 2025

Published 28 March 2025

10.1126/sciadv.adt9287